Surface stability of granular systems under horizontal and vertical vibration: The applicability of a coefficient of friction

P. J. King, Michael R. Swift, K. A. Benedict, and A. Routledge
School of Physics and Astronomy, University of Nottingham, Nottingham NG7 2RD, United Kingdom
(Received 22 May 2000)

We investigate the conditions under which the surface of a granular pile becomes unstable to vibrations. Three stability boundaries are identified, which depend upon the relative phase of the driving forces and the angle of the prepared slope. The experimental findings can be interpreted within the context of a Coulomb friction model and used to define an effective coefficient of friction. For up-hill motion we find that the coefficient of friction depends strongly on the slope angle and that, in general, it requires less vibration to transport grains uphill than would be otherwise expected.

PACS number(s): 45.70.Ht, 83.70.Fn

I. INTRODUCTION

A high proportion of industrial raw materials exist in the form of powders or grains and, at some phase of the production process, they are subjected to shaking and flow. Since the early work of Faraday on the behavior of granular systems under vibration [1], many studies have been conducted in this field. However, to date, we are only beginning to understand the wealth of dynamical physical properties exhibited by these materials [2–5].

Granular systems show a very wide range of behaviors under vibration, generally dependent upon parameters that include the coefficients of restitution of the grains and the vertical and horizontal acceleration of the system. For sinusoidal vibration, the latter can be conveniently expressed as $\Gamma_V = A_V\omega^2/g$ and $\Gamma_H = A_H\omega^2/g$, the ratios of the maximum accelerations resulting from the vibration to that of gravity. Here A_V and A_H are the amplitudes of vibration in the vertical and horizontal directions, respectively, and ω is the angular frequency. Solely under sinusoidal vertical excitation for which Γ_V somewhat exceeds unity, grains placed upon a vibrating surface may spontaneously form into conical piles [1]. If the grains are contained within a box, the system may break symmetry by forming shapes with tilted surfaces [3,6]; there is evidence that the presence of air is involved in the formation of these slopes [7]. Within the bulk of the material convective motion has been observed [1,8,9]. At higher values of $\Gamma_V(>2.5)$ the formation of arches and surface waves are evident [10,11] and in shallow layers of vibrating grains a wide range of patterns may be generated [12]. These arching, surface wave and pattern formation effects are enhanced by the removal of air. Grains confined in a box subjected to horizontal vibration alone also undergo convective flow [13].

Substantial simultaneous vertical and horizontal vibrations are applied to granular systems to produce conveyancing, an important transportation mechanism in a wide range of industrial processes. In theoretical treatments of conveyancing however, each grain is usually considered to interact in isolation with the vibrating surface and, if the vibration is sufficient for the grain to leave the surface, the subsequent collision is assumed to be completely inelastic so that the grain does not bounce [14–17]. The collective behavior of grains under both vertical and horizontal vibrations has not been widely considered. In particular, the conditions of vibration under which the surface of the granular arrangement loses stability have yet to be fully understood.

Recently Tennakoon and Behringer have studied the stability of granular surfaces to both vertical and horizontal vibration by observing ''self-piling'' [18]. Under certain conditions of vibration a granular system will spontaneously develop a slope, the angle of which increases with time until an equilibrium is reached. Tennakoon and Behringer measured this slope as a function of Γ_H, for a range of values of Γ_V, and in comparing their results with the predictions of a static friction model noted substantial deviations. Experimentally we find that measurements of this kind are often quite difficult to perform. The timescale for the approach to static equilibrium may be extremely long and the measurements are often affected by the motion ''jamming.'' The expected up-hill movement may cease at an early stage and not occur again until the apparatus is lightly tapped. The piling observed at higher values of Γ_H (for a given value of Γ_V) corresponds to a dynamic rather than a static equilibrium; the surface grains undergo a stick-slip motion during each cycle of the driving oscillation. The analysis of such a motion in terms of a friction coefficient is far more complex than modeling static equilibrium. Because of these difficulties we have chosen a different approach to investigate whether simple friction models may be applied to granular piles and have observed surface stability directly.

In the present paper we study the surface stability of sand and glass ballotini by applying horizontal and vertical vibration to prepared slopes, and investigating the vibrational conditions for the initiation of either up-hill or down-hill surface movement. We observe deviations from the predictions of the Coulomb friction model, which become more pronounced with increased frequency and with reduced grain size. At higher frequencies and for smaller grains it is notably easier to move grains up hill than the simple Coulomb model predicts. Our findings highlight the importance of collective dynamics at the onset of surface fluidization.

II. PREDICTIONS OF THE COULOMB MODEL

The Coulomb model of friction is well known. An object placed on a surface will remain stationary until a tangential

force F_T is applied that exceeds μF_N, where F_N is the normal force at the surface and μ is the coefficient of static friction. In a wide range of situations μ is observed to be only weakly dependent on the magnitude of F_N. An object will remain at rest on a surface inclined at an angle θ to the horizontal provided that $\tan(\theta) < \mu$ since on such a surface the forces F_T and F_N will be equal to $mg\sin(\theta)$ and $mg\cos(\theta)$, respectively. The same ideas have been applied to the surface stability of granular systems [18]. However, the surface is not homogeneous at the granular scale. A grain on a surface composed of similar grains lies in a local potential well formed by its neighbors and the depths of these wells are not in general identical. As the granular surface is slowly tipped to increasing angles, for example by inclining the container, the grains in the most shallow wells will fall down the slope to find a more secure position, or excite other grains from their own wells causing an avalanche. It is at first sight surprising that the angle at which major avalanching occurs, the static angle of repose θ_s, may be reproducibly measured, often to within about 1°. A granular ''coefficient of static friction'' may then be defined by $\mu = \tan(\theta_s)$. The question addressed here is the extent to which this coefficient may be used to estimate the surface stability of a granular system over a range of slope angles and under a range of dynamic situations where tangential and normal forces are applied through vibration.

Consider a granular slope of angle θ subjected to both a sinusoidal vertical vibration of amplitude A_V at an angular frequency ω and a sinusoidal horizontal vibration of amplitude A_H at the same frequency. We will restrict our study to situations in which the horizontal and vertical motions are either exactly in phase (+ phase) or 180° out of phase (− phase). In either case a surface grain that is stationary with respect to the surface is subjected to the force of gravity plus the forces from adjacent grains resulting from the vibration. Following Tennakoon and Behringer [18], let us first assume that it is the maximum forces due to the vibration that determine the conditions for surface stability. These maximum forces occur at times of maximum acceleration. The three force components on the grain are thus 1 downwards, Γ_V in a vertical direction, and Γ_H in a horizontal direction, when all forces are normalized by the force of gravity. Half a cycle later, peaks in the oscillatory forces will again occur but in the reversed direction. Thus for both the + phase and the − phase there are two points per cycle of peak force that will lead to slippage if the resolved tangential force F_T exceeds μF_N. These four situations are shown in Fig. 1.

The condition $F_T = \mu F_N$ leads to lines in the (Γ_V, Γ_H) plane that mark the boundary between stability and slippage. These are shown in Fig. 2. An upward arrow indicates the onset of slippage up the slope and a downward arrow indicates a boundary between stability and movement down the slope. The − phase boundary, resulting from force directions as in Fig. 1(a), is given by

$$\Gamma_H = \frac{\mu - t}{1 + \mu t}(1 - \Gamma_V), \tag{1}$$

where $t = \tan(\theta)$. The + phase boundary shown in Fig. 2 consists of an up-slope segment corresponding to Fig. 1(c),

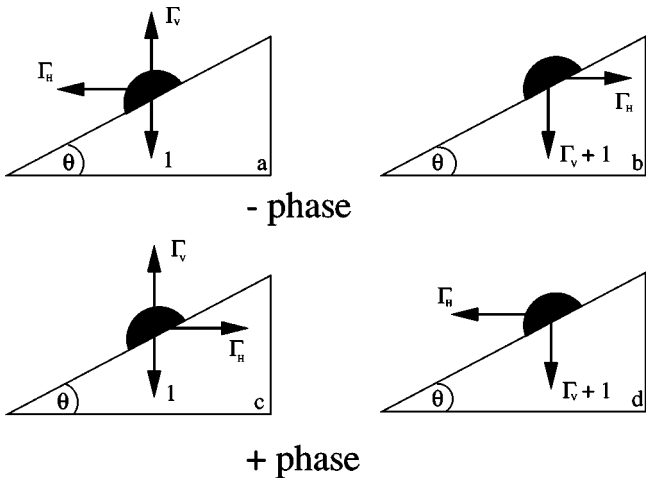

FIG. 1. The four situations that may lead to the onset of surface instability within the simple Coulomb model of friction; (a) and (b) correspond to ''−'' phasing of Γ_V and Γ_H, while (c) and (d) correspond to ''+'' phasing.

$$\Gamma_H = \frac{\mu + t}{1 - \mu t}(1 - \Gamma_V), \tag{2}$$

and a down-slope segment

$$\Gamma_H = \frac{\mu - t}{1 + \mu t}(1 + \Gamma_V), \tag{3}$$

corresponding to Fig. 1(d). The cusp at x is the transition between down-slope and up-slope movement. The resulting regions of stability in the (Γ_V, Γ_H) plane are shown for the − phase and the + phase as shaded regions in the insets to Fig. 2. The higher (broken) stability lines of Fig. 2, one of which corresponds to the force configuration in Fig. 1(b), are not relevant since stability has already been lost before these

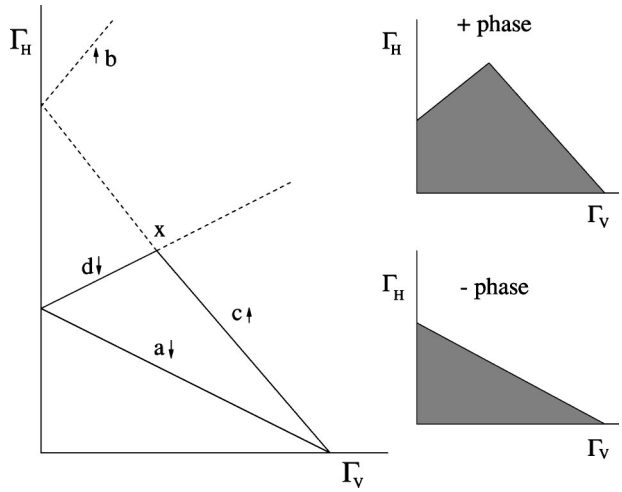

FIG. 2. The four stability boundary lines in the (Γ_V, Γ_H) plane corresponding to the four situations of Fig. 1. For clarity the regions of surface stability for the + phase and for the − phase are indicted by the shaded areas in the insets. The arrows indicate whether the slip that occurs just above each stability line is up-hill (↑) or down-hill (↓).

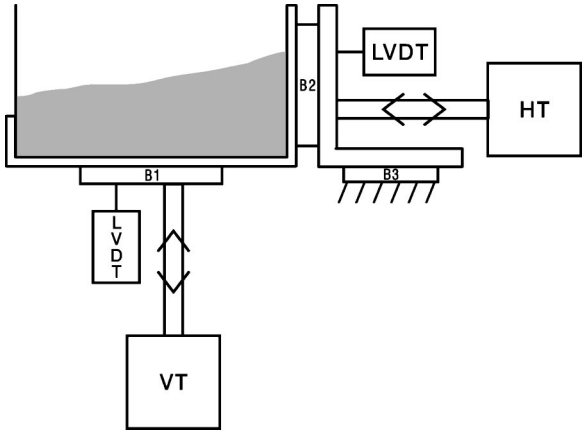

FIG. 3. A schematic diagram of the apparatus. The grains are contained within a detachable box that may be shaken vertically and horizontally by the two transducers VT and HT. The three precision ball slides B1, B2, and B3 ensure independent and accurately aligned movement. The vertical and horizontal motions are separately monitored by two LVDT's.

conditions are reached. It should be noted that at $\theta=0$ the boundary lines for the + and − phases coalesce to the form $\Gamma_H=\mu(1-\Gamma_V)$.

As shall be seen below, the experimentally determined stability lines do not intersect the Γ_H axis at $\Gamma_V=1$, but at a slightly higher value. To allow for this, we consider a generalization of the force model described above. Note that at any nonzero frequency, the maximum forces Γ_H and Γ_V are only applied fleetingly whereas a grain needs time to respond due to its inertial mass. To take this dynamical behavior into account, we consider a model in which the effective magnitude of the horizontal and vertical forces are each reduced by a factor $1/(1+\delta)$, where δ may be a function of frequency. Such a rescaling will shift the stability lines in the (Γ_V,Γ_H) plane, while leaving the slopes and structure of the diagram unchanged, i.e., the stability lines will be given by Eqs. (1), (2), and (3) with the 1 in brackets replaced by $1+\delta$. For a horizontal surface, this modification is equivalent to the correction parameter introduced empirically by Tennakoon and Behringer [18].

The validity of these simple models has been compared with experimental observations of surface stability made on a variety of granular materials with different slope angles and over a frequency range of 12.5 to 35 Hz.

III. EXPERIMENTAL METHODS

The experiments were conducted on grains contained within a perspex (PMMA) box of internal width 11 mm, length 50 mm, and depth 50 mm. Preliminary tests showed that it was necessary to roughen the bottom of the box, or to fill the box to a depth exceeding about 6 mm, to avoid probing slippage between the bottom of the box and the granular system. Our measurements have been conducted with depths of 20 mm–30 mm, for which the first slippage is always at the free surface of the grains. The box may be vibrated both along the horizontal and vertical axes by two transducers, the motions being constrained by precision ball slides (Fig. 3). The horizontal and vertical box motions are monitored by two linear voltage-displacement transducers (LVDT's), which enable the horizontal and vertical amplitudes, the relative phase, and any deviations from sinusoidal motion to be detected. In these experiments the deviations from sinusoidal motion are negligible and the uncertainty in the phase difference is always less than 15°. The majority of the experiments have been conducted in an atmosphere of ambient air. Although some authors have noted that air effects are not to be expected in surface stability experiments [18], we have carried out tests using boxes evacuated to below <0.5 Torr and observe that the presence of air does in fact somewhat modify the surface stability, as we shall report below.

Horizontal granular surfaces have been prepared by the application of substantial horizontal motion $\Gamma_H>2$, the amplitude of which is then slowly reduced. Slopes of various angles have been prepared by the piling resulting from substantial vertical vibration in the presence of air using $\Gamma_V>3$ alone, or with the addition of a smaller horizontal component. Care has been taken to set up slopes that were of constant angle throughout the region of observation, the central section of the box. The onset of surface motion has been observed with the eye and through a low power optical microscope using light reflected from individual grains. Under vibration these reflections become streaks and it is the movement of these streaks that we observe. It is helpful, whenever possible, to angle the axis of the microscope so that it lies approximately parallel to the motion of the vibration at the point of slippage. Most of the measurements have been carried out on sand or glass ballotini. The silica sand is of irregular shape and has dimensions that lie in the range 300–800 μm. In its history it has been weathered sufficiently to somewhat blunt the sharpest edges. The glass ballotini are of dimensions 75–150 μm, 180–300 μm, or 425–600 μm and are close to spherical in shape. The sand and ballotini self-pile in air under vertical vibration alone, the larger ballotini more slowly than the sand or smaller ballotini.

IV. OBSERVATION OF SLIPPAGE ON HORIZONTAL SURFACES

Figure 4 shows the stability line observed on a freshly created horizontal surface of glass ballotini of 180–300 μm diameter vibrated at 25 Hz. If Γ_V is set to a low value and Γ_H is slowly increased (e.g. along the path α in Fig. 4) the first sign of surface activity involves an occasional grain chattering in a particularly shallow well. At a slightly higher value of Γ_H these few grains break loose and move on the surface until they find a more secure well and again become stationary. Close to the stability line indicated in Fig. 4, a substantial fraction of the surface grains are chattering and an appreciable minority have broken loose at any time, in apparently random directions. Individual grains may come to rest or may hit other grains to form local avalanches. Just above the stability line most of the grains are observed to be undergoing apparent random motion. The onset of surface motion is slightly hysteretic; once motion has begun Γ_H must be decreased somewhat below the stability line for motion to cease.

It is clear that, on the basis of visual inspection and in the presence of hysteresis, the position of the ''stability line'' is difficult to define precisely. We have used the criterion that,

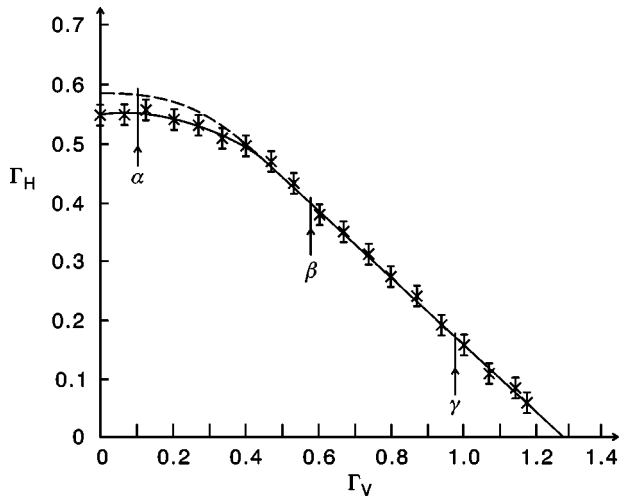

FIG. 4. The boundary of stability in the (Γ_V,Γ_H) plane for a horizontal surface of 180–300 μm diameter ballotini vibrated at 25 Hz. The broken line corresponds to a surface after ''aging'' and the routes α, β, and γ are discussed in the text.

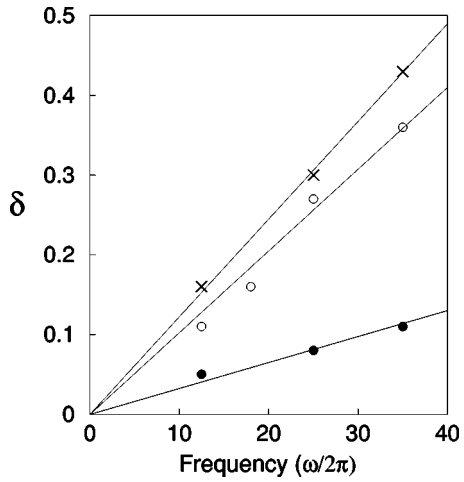

FIG. 5. The parameter δ plotted as a function of frequency (Hz) for ballotini of dimensions 75–150 μm (crosses), 180–300 μm (open circles), and 425–600 μm (filled circles).

for a given Γ_V, the stability line lies at the lowest value of Γ_H for which all of the surface grains will move within a time scale of one minute; on this criterion it certainly falls within the ''error bars'' indicated.

If Γ_V is set to an intermediate value, e.g., $\Gamma\sim 0.5$, and Γ_H is again slowly increased (path β in Fig. 4) similar events occur, but the motion of the grains close to and above the stability line is less random, consisting of some apparently random jostling superimposed upon an obvious overall motion in a direction dictated by the relative phase of the vertical and horizontal vibration. As Γ_V approaches or just exceeds unity, and Γ_H is again slowly increased (path γ in Fig. 4) very little surface jostling is observed at the stability line. Rather the surface slips as a whole, the slippage extending for a number of grain diameters below the surface. For Γ_V values greater than unity it might be expected that the floor of the box would separate from the grains as the box accelerates faster than the grains can fall under gravity. However, for those parts of the stability line with $\Gamma_V>1$, we observe that the only motion of the grains relative to the box takes place close to the upper surface. Thus the nature of the instability varies with the magnitude of Γ_V, from individual grain movement at low values, through slippage just below the surface, to deeper slippage at higher values of Γ_V.

The plateau region observed in the low Γ_V part of the stability diagram is far more susceptible to ''aging'' than other regions. If an appreciable $\Gamma_V<1$ is applied for a period of time to a newly created surface, or surface motion is repeatedly induced and then stopped, the plateau region of the stability line is displaced to somewhat higher values of Γ_H as is shown by the broken line in Fig. 4. However, we have been unable to remove the plateau region completely.

In comparing the observed stability behavior with the prediction $\Gamma_H=\mu(1-\Gamma_V)$ of the unmodified Coulomb friction model, a number of features are evident. Despite the changing nature of the surface slippage at different values of Γ_V, the observed stability boundary is very close to a straight line in the (Γ_V,Γ_H) plane over most of the range of Γ_V. In particular, there is no appreciable deviation from straight-line behavior as the instability passes from surface movement to slippage that extends well below the surface. However, two features indicate deviations from the simple model. Firstly, at low values of Γ_V, the observations deviate from straight-line behavior, with Γ_H at the stability line becoming independent of Γ_V as the plateau shown in Fig. 4 indicates. Secondly, Γ_H does not become zero at $\Gamma_V=1$ as the simple model suggests, but at a higher value, $\Gamma_V=1+\delta$. In Fig. 4, δ is equal to 0.28. A similar effect has been reported by Tennakoon and Behringer in measurements on Ottawa sand [18]. For this reason we introduced above the modified friction model in which the strength of Γ_H and Γ_V are reduced by a factor of $1/(1+\delta)$. The zero-slope stability line then becomes $\Gamma_H=\mu(1+\delta-\Gamma_V)$. We will investigate the ability of this two-parameter model to describe surface stability in a range of granular materials under different driving conditions and slope angles.

We have measured the $\theta=0$ stability lines for three sizes of ballotini, 75–150 μm, 180–300 μm, and 425–600 μm, and at frequencies of 12.5 Hz, 25 Hz, and 35 Hz. For each system considered, the quality of the data is comparable to that shown in Fig. 4. We observe that the stability line is straight over most of its span despite the nature of the failure of stability passing from the surface to the bulk. Consequently we have been able to extract values of δ and the gradient $-\mu$ for each of the systems and the results are shown in Figs. 5 and 6. It may be seen that, within the errors of the experiment, δ increases linearly with frequency, and is larger for smaller grains. The coefficient of friction deduced from these measurements is also a function of frequency, increasing as the frequency is lowered. This frequency dependence is stronger for smaller grains. For each grain size, μ may be extrapolated to a zero frequency value of 0.80 ± 0.02. It is not surprising that the extrapolated values are very similar, since the ballotini are all of the same shape and each sample spans a similar range of dimensions. This extrapolated value is in excellent agreement with measurements obtained from the static angle of repose, which lie within the range 0.78 ± 0.04.

These stability experiments have been repeated on sand,

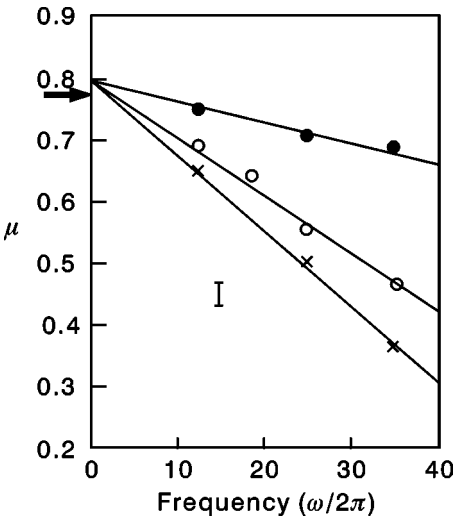

FIG. 6. The coefficient of friction μ, deduced from measurements on horizontal surfaces, plotted as a function of frequency (Hz) for ballotini of dimensions 75–150 μm (crosses), 180–300 μm (open circles), and 425–600 μm (filled circles). The value of μ corresponding to the static angle of repose is indicated by an arrow.

giving similar results. Again δ is linearly dependent upon frequency and the values of μ at frequencies of 12.5, 25, and 35 Hz may be extrapolated to obtain a zero-frequency coefficient that is in agreement with the coefficient of friction extracted from measurements of the static angle of repose (1.01 ± 0.05).

We have repeated the experiments of Fig. 4 in a box that was evacuated to below 0.5 Torr; at these pressures the viscous air damping is severely reduced [19]. As Γ_H is increased along the path α, the chattering is enhanced by the removal of the air and the avalanches are more extensive, the granular motion being clearly more lively. Along paths β and γ motion also occurs at lower values of Γ_H. The effect on the stability line is to lower its position throughout by about $\Delta\Gamma_H = 0.1$. While the form of the plateau and the value of μ are very little changed, the value of δ is approximately halved by the removal of air. It thus appears likely that δ is determined by damping. The higher values of δ for smaller sized grains are also consistent with this conclusion.

V. OBSERVATION OF SLIPPAGE ON SURFACES OF NONZERO SLOPE

We have carried out detailed observations of surface slippage using ballotini of dimensions 180–300 μm, slopes of $\tan(\theta) = 0.1$, 0.2, 0.3, 0.4, and 0.46, and a frequency of 25 Hz. We investigate the limits of stability for both the + phase and the − phase in air. The results for $\tan(\theta) = 0.2$ are shown in Fig. 7(a) and for $\tan(\theta) = 0.4$ in Fig. 7(b). In each case the stability lines have much in common with the predictions of the simple Coulomb friction model shown in Fig. 2. The low Γ_V plateau observed at $\theta = 0$ has largely disappeared by $\tan(\theta) = 0.1$ and is completely absent for the larger angles of Figs. 7(a) and 7(b).

As expected the − phase stability boundary has the form of a single straight line and when stability is lost, the motion is down hill. The surface motion at low Γ_V consists of near random jostling with a small average down-hill component,

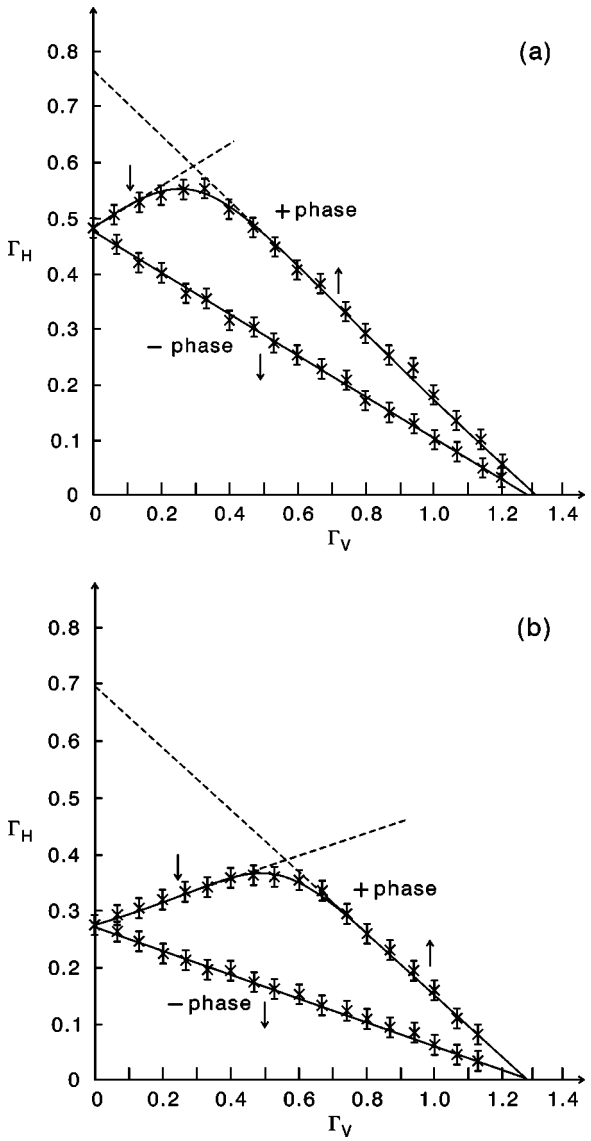

FIG. 7. The boundaries of stability in the (Γ_V, Γ_H) plane for a sloping surface of 180–300 μm diameter ballotini vibrated at 25 Hz: (a) $\tan(\theta) = 0.2$ and (b) $\tan(\theta) = 0.4$. In each diagram the lower data is for the − phase and the upper data is for the + phase. The arrow ↑ indicates the boundary between surface stability and up-hill motion while the arrow ↓ indicates the boundary between surface stability and down-hill motion.

passing to a collective motion down hill as higher values of Γ_V are applied, with deeper layers involved. The + phase stability line has two sections, a down-hill section at low Γ_V, and at higher values of Γ_V, a straight up-hill section. For those slope angles free of the low Γ_V plateau $[\tan(\theta) > 0.15]$, and to within experimental error, the + phase down-hill section is the extension of the down-hill − phase line reflected about $\Gamma_V = 0$, as the Coulomb friction model predicts. While the simple model suggest an abrupt change of slope at the boundary between the two (x in Fig. 2), experimentally the cusp is rounded. For the down-hill section the surface motion following the loss of stability consists of near random jostling with a small average down-hill component. As Γ_V is increased, the down-hill motion becomes more collective. In the up-hill section the motion again be-

TABLE I. The coefficient of friction μ deduced from the stability conditions for surfaces at various tilt angles. The values of μ for positive $\tan(\theta)$ are estimated from the boundary between stability and down-slope motion, while the values for μ for negative $\tan(\theta)$ are estimated from the boundary between stability and up-slope motion.

Slope angle $\tan(\theta)$	Ballotini 180–300 μm 25 Hz	Sand 300–800 μm 25 Hz	Sand 300–800 μm 12.5 Hz
0.46	0.70		
0.4	0.67	1.15	1.03
0.3	0.64	1.12	1.00
0.2	0.62	1.05	1.05
0.1	0.57	1.04	1.03
0.0	0.55	1.03	1.05
−0.1	0.46	0.97	1.06
−0.2	0.35	0.87	1.01
−0.3	0.23	0.79	1.01
−0.4	0.11	0.73	0.91
−0.46	−0.02		

comes increasingly collective as higher values of Γ_V are applied, but with a greater jostling component than for down-hill motion. At these high values of Γ_V, localized regions of the surface are observed to ''melt'' and ''resolidify,'' corresponding to up-hill avalanches.

In interpreting the detailed form of our stability diagrams we note that, within the experimental error, the + phase and − phase stability lines intercept the horizontal axis at the same value of $\Gamma_V = 1 + \delta$ *irrespective of the angle used*. The observed intercepts are thus consistent with the modified model, with δ being independent of the slope. The gradients of the stability boundaries may be used to deduce values of the coefficient of friction μ for the various slope angles and for down-hill and up-hill movement. These are shown in Table I. It is convenient to offer $\mu(\theta)$ for positive and negative angles, the positive angles corresponding to the boundaries of down-hill movement [deduced from Eq. (1)] and the negative angles corresponding to the boundaries of up-hill movement [deduced from Eq. (2)].

It may be seen that the coefficient of friction of the 180–300 μm ballotini measured at 25 Hz is a strong function of slope angle, particularly for the + phase for which μ reduces dramatically with angle. At higher angles, as the static angle of repose is approached, it actually reaches zero to within the observational error. Experimentally, the limits to up-hill granular movement for any particular value of Γ_V, lie at a lower value of Γ_H than predicted by the model, with μ determined from static measurements alone. It requires less vibration to move grains up hill than is expected. Data is also shown for 300–800 μm sand measured at 25 Hz. We observe a dependence of μ upon θ; again it is easier to push grains up hill than predicted. However for these larger grains the variation of μ with angle is less pronounced. Finally we present data for sand taken at the lower frequency of 12.5 Hz. It may be seen that in this case μ is essentially independent of angle except for up-hill motion at the highest angle measured. This constant value is consistent with the coefficient of friction obtained from the static angle of repose. It is clear that the effective coefficient of friction deduced from surface stability measurements and the Coulomb friction model is, in general, dependent upon both frequency and slope angle. However, it becomes less dependent upon angle at lower frequencies and for larger grains, the situations for which the data of Figs. 5 and 6 indicate the closest approach to the static limit.

VI. DISCUSSION

Knowledge of the conditions under which a system of grains is stable to both horizontal and vertical vibration is extremely important in very many practical situations. Our studies have shown that the nature of the surface instability varies with the magnitude of Γ_V, passing from instability to jostling motion with a large random component at lower values of Γ_V, to instability to collective motion at higher values of Γ_V, with deeper layers being involved. It is clear from our observations that stability failure involves the complex dynamic motion of the grains resulting from the vibrations of their neighbors. It is influenced by damping, both due to inelastic collisions and the viscous nature of air. These effects lead to apparently random motion at the surface (low Γ_V) or to surface layers flowing over the underlying grains with little relative motion within a layer (higher Γ_V).

Simple additional experiments have been conducted to investigate the motion of a free 4-mm-diameter steel ball resting upon a close-packed layer of similar balls, which have been glued into position on a horizontal plate. The plate was then vibrated vertically and horizontally at 25 Hz. As Γ_H is very slowly increased at low Γ_V, the free ball is observed to begin chattering within its well. The amplitude of the chattering increases and eventually the ball is thrown out of the well, in no particular direction. This is consistent with the chattering and random motion found along path α of Fig. 4. The overall stability diagram for such a steel ball is in fact remarkably similar to that of the collection of grains of Fig. 4, exhibiting the flat plateau at low Γ_V, and straight line behavior at higher Γ_V. The value of δ is nonzero, and depends upon how the static balls are mounted.

For our granular systems it is noteworthy that the stability boundaries in the (Γ_V, Γ_H) plane are usually straight lines over wide ranges of the variables, the exceptions being the plateaus found at low Γ_V for θ close to zero, and the rounded cusps between the up-hill and down-hill sections of the + phase stability lines. With these exceptions the boundaries are of the form $a\Gamma_V + b\Gamma_H = 1$, where a and b are parameters that depend upon the given slope angle, phase, and driving frequency. This linearity is sufficient to ensure that the stability conditions may be described by resolving forces into tangential and normal components and by using a ''coefficient of friction.'' The success of the static Coulomb friction model in predicting the overall structure of the stability diagram is apparent. However, the simple model has two failings: (1) the coefficient of friction is observed to depend upon frequency, slope angle, and phase, and (2) the boundary lines are such that when $\Gamma_H = 0$, $\Gamma_V = 1 + \delta$, where δ is dependent upon frequency and grain type but not upon angle or phase.

Due to the fluctuating rather than static nature of the surface, an empirical model in which the effectiveness of both

Γ_H and Γ_V is reduced by a factor of $1/(1+\delta)$, has been used. This parametrization was chosen so that all the nontrivial angular dependence of the stability boundaries is contained within $\mu(\theta)$. It is also possible to consider different reduction factors for Γ_H and Γ_V, and to treat these as independent parameters, rather than allowing μ to vary. We have fitted the experimental data to this type of behavior but find that no new physical insight is gained from such a model. Note that, whatever parametrization is used to describe the system, the observations do correctly recover the static limit as the frequency is lowered. The key to understanding the frequency and phase dependence of the parameters lies in the detailed dynamics of the granular material. This includes the chattering movement within local potential wells and the damping that results from collisions and from the surrounding fluid.

Finally, we return to the self-piling experiments of Tennakoon and Behringer [18]. We have carried out experiments of this type on both sand and ballotini. We find that the static slopes obtained under the application of Γ_H and Γ_V are consistent with the up-hill stability branch of our measurements, allowing for the small errors in performing the experiments, and the differences in the definition of ''stability.'' In the Tennakoon and Behringer experiments an attempt is made to obtain static stability, waiting, in principle, until the ''last'' grain has moved. In our own experiments we have judged the stability lines to be at the least values of Γ_H and Γ_V where all grains move within the time scale of a minute. Nevertheless the agreement is acceptable. However, we have now established that the effective coefficient of friction is a function of angle, varying more strongly with angle at higher frequencies. This dependence has not been allowed for by Tennakoon and Behringer, and no doubt contributes to the discrepancies between theory and experiment noted by these authors.

ACKNOWLEDGMENTS

We would like to thank R.M. Bowley for very helpful discussions and to acknowledge the excellent engineering skills of D. Holt.

[1] M. Faraday, Philos. Trans. R. Soc. London **52**, 299 (1831).
[2] For a review see H. M. Jaeger, S. R. Nagel, and R. P. Behringer, Rev. Mod. Phys. **68**, 1259 (1996).
[3] P. Evesque, Contemp. Phys. **33**, 245 (1992).
[4] R. P. Behringer, Int. J. Bifurcation Chaos Appl. Sci. Eng. **7**, 963 (1997).
[5] L. P. Kadanoff, Rev. Mod. Phys. **71**, 435 (1999).
[6] P. Evesque and J. Rajchenbach, Phys. Rev. Lett. **62**, 44 (1989).
[7] H. K. Pak, E. Van Doorn, and R. P. Behringer, Phys. Rev. Lett. **74**, 4643 (1995).
[8] K. M. Aoki, T. Akiyama, Y. Maki, and T. Watanabe, Phys. Rev. E **54**, 874 (1996).
[9] J. B. Knight, E. E. Ehrichs, V. Yu. Kuperman, J. K. Flint, H. M. Jaeger, and S. R. Nagel, Phys. Rev. E **54**, 5726 (1996).
[10] S. Douady, S. Fauve, and C. Laroche, Europhys. Lett. **8**, 621 (1989).
[11] C. R. Wassgren and C. E. Brennen, Trans. ASME, J. Appl. Mech. **63**, 712 (1996).
[12] F. Melo, P. Umbanhowar, and H. L. Swinney, Phys. Rev. Lett. **72**, 172 (1994); **75**, 3838 (1995); E. Clément, L. Vanel, J. Rajchenbach, and J. Duran, Phys. Rev. E **53**, 2972 (1996); L. S. Tsimring and I. S. Aranson, Phys. Rev. Lett. **79**, 213 (1997).
[13] M. Medved, D. Dawson, H. M. Jaeger, and S. R. Nagel, Chaos **9**, 691 (1999).
[14] J. H. Booth and H. McScallion, Proc. Inst. Mech. Eng. **178**, 521 (1963).
[15] R. M. Nedderman and G. H. L. Harding, Trans. Inst. Chem. Eng. **68A**, 124 (1980).
[16] K. L. Ng, L. A. Ang, and S. C. Chng, Proc. Inst. Mech. Eng., Part C: Mech. Eng. Sci. **200**(B2), 123 (1986).
[17] E. M. Sloot and N. P. Kruyt, Powder Technol. **87**, 203 (1996).
[18] S. G. K. Tennakoon and R. P. Behringer, Phys. Rev. Lett. **81**, 794 (1998).
[19] S. G. K. Tennakoon, L. Kondic, and R. P. Behringer, Europhys. Lett. **45**, 470 (1999).